

# Static, Modal and Buckling Analyses of Automotive Propeller Shaft using Finite Element Methods

Mukul Kumar and Nilamber Kumar Singh\*

Design Engineering, National Institute of Technology Patna, INDIA

\*Corresponding author E-mail: nilambersingh@nitp.ac.in

**Abstract.** This paper presents a comparative study of static, modal and buckling analyses of aluminium alloys and steel, Al6351, Al7075 and SM45C made automotive propeller shafts using finite element methods. The 3D-model of propeller shaft is created in CATIA and then analysis is done using ANSYS. Natural frequency is determined for six different mode shapes and the critical load at which the propeller shaft starts buckling is compared for dissimilar materials. The stress distribution and unsafe areas are shown for the modification in existing design of the propeller shaft. It is found that the aluminum propeller shaft has higher natural frequency than the steel propeller shaft. Therefore, the resonance stage reaches later in aluminum propeller shaft and enhances its life.

## 1. Introduction

The propeller shaft (drive shaft) is an important mechanical component of an automotive drive line system which is used to transmit the engine torque to the drive wheels so that the vehicle can move. Transmission of this torque must be smooth and uninterrupted for continuously running the vehicle. The efficiency of the propeller shaft depends on its weight, critical speed and the vibration characteristics such as natural frequency and mode shape. Therefore, the efficient design of the shaft is a crucial issue as it has limitation on these parameters. There are many researchers working on the modification and implementation of the propeller shaft design. Lee *et al.* [1] designed a one-piece automotive hybrid aluminium-composite propeller shaft and found that the weight of the hybrid shaft reduced to one-fourth whereas the torque transmission capability increases 1.6 times as compared to the conventional steel automotive propeller shaft. Finite element analysis is done by Talibet *et al.* [2] to design composite automotive drive shafts of carbon-epoxy and glass-epoxy fiber with an epoxy matrix. Cho *et al.* [3] used aluminium tube and carbon fiber-epoxy to manufacture one piece automotive drive shafts. Manjunath *et al.* [4] developed particle swarm algorithm programming for optimum design of the lightweight propeller shaft. Pater *et al.* [5] performed the numerical and experimental results of producing hollow parts by a new method of rotary compression. Rao *et al.* [6] used carbon reinforced plastics and glass fiber reinforced plastics to design a hollow propeller shaft for automobile using FEA technique. The fatigue behaviour of a hybrid aluminium and composite materials propeller shaft is studied by Khalid *et al.* [7]. Zhang *et al.* [8] investigated the instability and vibration of a propeller shaft system. Rangaswamy *et al.* [9] designed and analyzed a one-piece rear wheel composite drive shaft for maximum power transmission applications in passenger cars by using FEA technique. The aim of this paper is to design a lightweight weight and high strength automotive propeller shaft to maximize the torque transmission and buckling capability by minimizing vibration and noise. The propeller shaft must be capable to operate at different speeds and load conditions by constantly changing relative angles between transmission and axle while transmitting the torque.



## 2. Materials

Material selection plays a vital role in product design and development. The aluminum alloy is suitable for propeller shaft applications under all loadings and vibration conditions due to low density, lightweight, strong at low temperature, good heat conductor and excellent corrosion resistance. The physical and mechanical properties [1,10,11], and the chemical compositions [12-14] of the selected materials, Al6351, Al7075 and SM45C are given in Table 1 and Table 2 respectively.

**Table 1.**Physical and mechanical properties of materials

Materials	Density (kg/m <sup>3</sup> )	Poisson's ratio	Elastic modulus (MPa)	Shear modulus (MPa)	Shear strength (MPa)
Al6351	2740	0.33	72000	27000	207
Al7075	2810	0.33	71500	27000	330
SM45C	7600	0.3	207000	80000	370

**Table 2.**Chemical compositions of materials in wt.%

Materials	Al	Si	Mg	Mn	Fe	Ti	Zn	Cu	Cr	P	S	C	Ni
Al6351	95.36	1.30	1.0	1.0	0.60	0.20	0.10	0.10	0.25	-	-	-	-
Al7075	87.32	0.40	2.9	0.30	0.50	0.20	6.1	2.0	0.28	-	-	-	-
SM45C	-	0.25	-	-	98.84	-	-	-	0.20	0.03	0.03	0.45	0.20

## 3. Theory

An automotive drive line is an assembly of propeller shaft (long drive shaft), universal joints and slip joints, final drive, differential assembly and axle shaft (short drive shaft). It is used to transfer the engine torque from the transmission output shaft to the drive wheels (rear or front) so that the vehicle can move. It provides smooth and uninterrupted transfer of power from engine to rear axle to move the vehicle with more effectively. The propeller shaft is the shaft by means of which drive is given to the driving axle. Since the propeller shaft has to withstand many torsional loads, it is usually made of tubular cross-section. The shafts are made of steel, aluminium or composite materials. It is made either in one piece or in two pieces. In one piece propeller shaft, the drive transmitted to the differential of the rear axle by a long one piece propeller shaft. This type of propeller shaft has universal joints at each end. In vehicles having long wheel base such as truck and buses, the propeller shaft is in two pieces and is supported at the centre to avoid whipping action of a long shaft. In the centre, a third universal joint between the two shafts and a centre bearing to support the middle of the shaft assembly is provided. The rubber rings are used on the centre bearing to take care of the angular movement of shaft and also to absorb vibrations. The two pieces propeller shaft increases the overall weight of the vehicle and hence, is not desirable in today's market. The lightweight propeller shaft having high strength and minimum possible cost is always the goal of a design engineer. The bumpy road surfaces or other similar driving conditions can result in deviation in relative position of the differential and the wheels or axles. It is therefore crucial that the propeller shafts can compensate for this positional shift, ensuring that the engine torque is transferred smoothly to the wheels. For this reason, the propeller shafts are provided with slip joints (or sliding joints) which enables the propeller shaft to adjust for the change in length. The splined end of the shaft slides inside of the other end to increase or decrease in length.

## 4. Results and Discussions

The 3D CATIA models of aluminium alloys and steel, Al6351, Al7075 and SM45C made propeller shafts are imported to ANSYS workbench to analyse the stress and strain distribution on the shafts, natural frequencies at different mode shapes and buckling loads at which the structures become

unstable. The numbers of tetrahedral elements in the meshing of these models are 20592, 19014 and 26736 respectively, whereas the numbers of nodes are respectively 41255, 37781 and 51578 for all analyses (static, modal and buckling) using same boundary conditions. The boundary conditions are: one end of the propeller shaft constraints from all directions and the torque 3500Nm [1] is applied on the other end. The outer and inner diameters of the propeller shaft are 72 mm and 52 mm respectively whereas its length is taken as 1500 mm [15]. The propeller shaft is assumed to rotate at a constant speed about its longitudinal axis. The shaft is uniform and perfectly balanced. All non-linear and damping effects are neglected.

#### 4.1. Static-structural analysis

The static analysis is used to determine forces, displacements, stresses and strains in structures and their components under static loading conditions. The analytical and simulated results are presented in Table 3. The maximum shear stress and von-Mises stress are found at the outer side and the minimum shear stress and von-Mises stress are found at the inner side of the hollow propeller shaft on its free end. The total deformation is maximum at fixed end and minimum at the free end on which the torque is applied. The weight of the aluminum propeller shaft reduced by 64% as compared to the steel propeller shaft. Here, the von-Mises stresses are determined by ANSYS simulation only for different materials. Figure 1 shows von-Mises stresses in the Al6351 propeller shaft at its different sections. Similar distributions of stresses and deformation are found on propeller shafts of other materials.

**Table 3.** Analytical and simulation results of static analysis

Materials	Mass (kg)	Maximum shear stress (MPa)		Maximum deformation (mm)		Von-Mises stress (MPa)
		Analytical	ANSYS	Analytical	ANSYS	ANSYS
Al6351	8.004	65.607	66.638	3.533	3.636	115.42
Al7075	8.209	65.607	66.736	3.558	3.633	115.59
SM45C	22.204	65.607	66.619	1.216	1.236	115.39

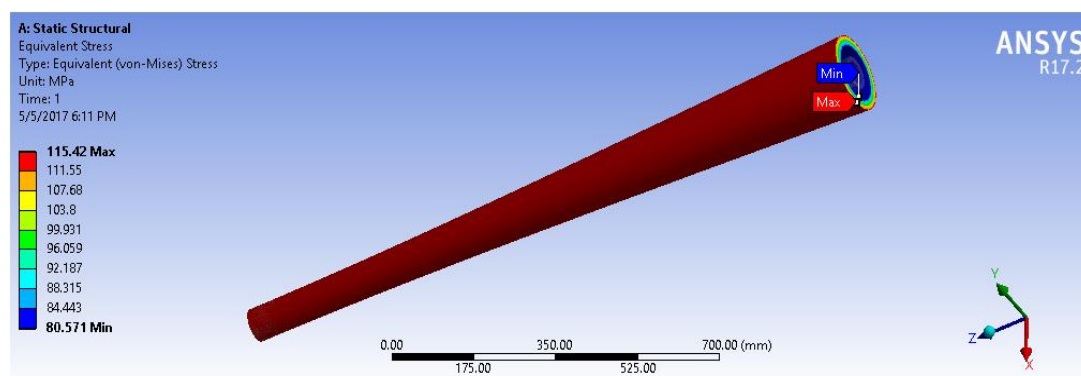


**Figure 1:** Equivalent (von-Mises) stresses on Al6351 propeller shaft

#### 4.2. Modal analysis

Modal analysis is done on the aluminum alloys and steel propeller shafts to find its natural frequencies and their respective mode shapes. No load is applied on the propeller shaft except boundary conditions by assuming it fixed at one end and torque is applied on other free end of propeller shaft. Table 4 shows the results of analytical and ANSYS simulation of Al6351, Al7075 and SM45C propeller shafts at six different mode shapes when boundary conditions are applied. It is found that the aluminum propeller shaft has higher natural frequency than the steel propeller shaft. Therefore, the resonance stage reaches later in aluminium propeller shaft and enhances its life. The aluminium structures are

preferably used in mechanical operations under free vibration conditions. Figure 2 shows the total deformation of Al6351 propeller shaft at sixth mode. Similar distribution of deformations is found in other materials. The maximum natural bending frequency is found at minimum deformation whereas the minimum natural frequency is found at maximum deformation. The maximum stress point and unsafe areas are obtained by deformation produced during the modal analysis of the propeller shaft and thereafter, similar distributions of natural frequency *versus* total deformation are found on the shafts of selected materials. The natural bending frequency depends on length, thickness, diameter and material specific stiffness of the hollow propeller shaft.

**Table 4.** Analytical and simulation results of modal analysis

Mode	Natural frequency (Hz) (Al6351)		Natural frequency (Hz) (Al7075)		Natural frequency (Hz) (SM45C)	
	Analytical	ANSYS	Analytical	ANSYS	Analytical	ANSYS
1	28.32	28.224	28.84	28.784	27.87	27.87
2	28.32	28.225	28.84	28.784	27.87	27.87
3	177.56	173.94	180.76	177.4	174.68	171.78
4	177.56	173.94	180.76	177.4	174.68	171.78
5	496.61	474.8	505.21	484.37	488.20	468.94
6	496.61	474.8	505.21	484.38	488.20	468.95

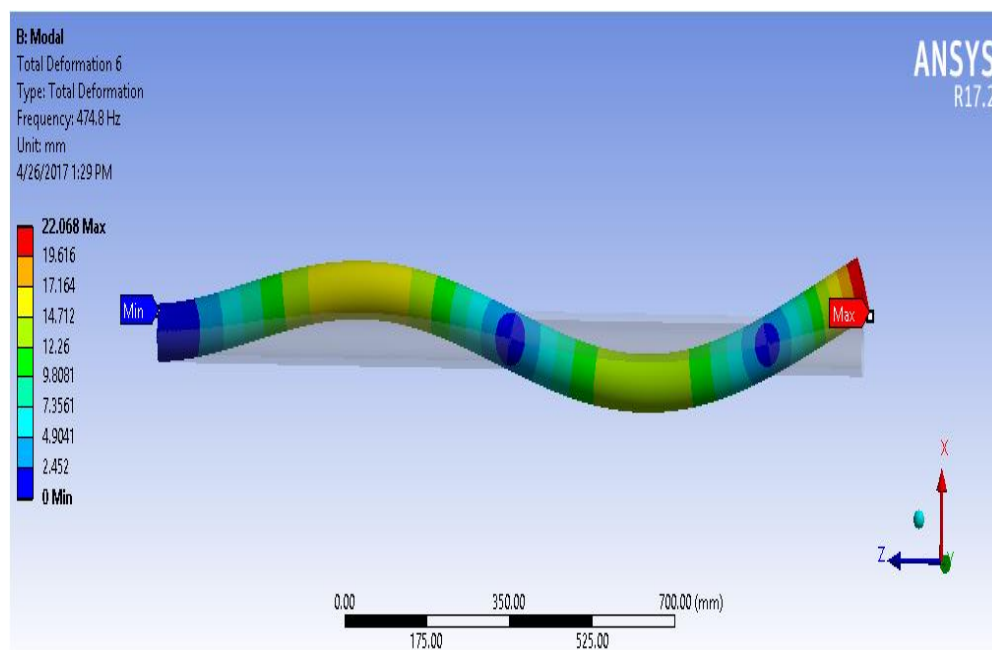


**Figure 2:** Deformation of Al6351 propeller shaft under sixth mode vibration

#### 4.3. Buckling analysis

Torsional buckling capacity of the shaft is determined as:

$$\text{Torsional buckling capacity (Analytical): } T_b = \tau_{cr} \times 2\pi r^2 t \quad (1)$$

$$\text{Where critical Torsional critical stress: } \tau_{cr} = \frac{E}{3\sqrt{2}(1-\nu^2)^{3/4}} \times \left(\frac{t}{r}\right)^{3/2} \quad (2)$$

$$\text{Torsional buckling capacity (ANSYS): } T_b = \text{load multiplier} \times \text{transmitter torque} \quad (3)$$

Where,  $T_b$  = Torsional buckling capacity (N-mm),  $\tau_{cr}$  = Shear critical stress (N/mm<sup>2</sup>),  $E$  = Young's modulus (GPa),  $t$  = thickness of shaft (mm),  $L$  = length of shaft (mm),  $r$  = mean radius and  $\nu$  = Poisson's ratio.

The magnitude of buckling load that causes buckling and associated buckling mode shapes are determined in linear buckling analysis using finite element methods (FEMs). The FEM technique provides the calculations of a large number of buckling modes and the associated buckling load factors (BLF) and multiplied with transmitted torque to get the torsional buckling capacity. The buckling mode presents the shape of structures when the structure buckled in a particular mode shape but says nothing about the numerical values of stresses and displacements. Table 5 shows the analytical and simulated results of buckling analysis of the propeller shaft of selected materials. Figure 3 shows the shape of Al6351 propeller shaft when it buckled in a particular mode shape and obtained the load multiplier 60.167 at which total deformation is maximum. Similar distributions of buckling load are found on the propeller shafts of Al7075 and SM45C materials. The simulated results agree well with the theoretical results.

**Table 5.** Analytical and simulation results of buckling analysis

Materials	Torsional Buckling capacity (N-mm) (Analytical)	Torsional Buckling capacity (N-mm) (ANSYS)
Al6351	$2.04 \times 10^5$	$2.10 \times 10^5$
Al7075	$2.03 \times 10^5$	$2.179 \times 10^5$
SM45C	$1.493 \times 10^5$	$1.435 \times 10^5$

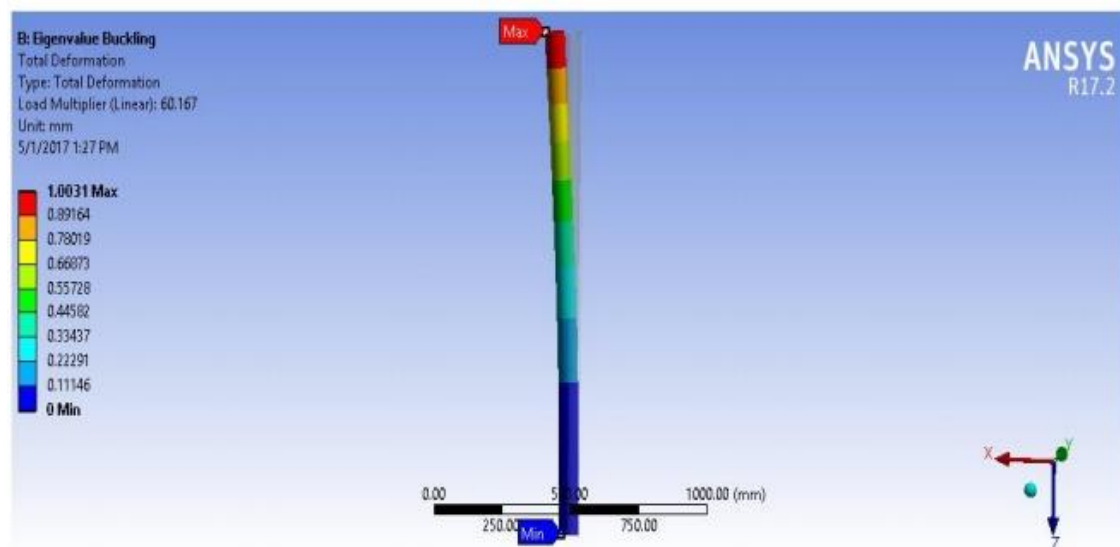


**Figure 3:** Deformation of Al6351 propeller shaft during buckling

## 5. Conclusions

The following conclusions can be drawn from the present work:

- The maximum shear stresses developed in Al6351, Al7075 and SM45C propeller shafts are lower than the shear strengths of the respective materials, and therefore the design of the propeller shaft will be safe under steady loading conditions.

- The weight of the aluminum propeller shaft reduced by 64% as compared to the steel propeller shaft. This will increase the fuel efficiency of the automobile vehicles having aluminum propeller shaft.
- Natural frequency of the aluminum propeller shaft is higher than that of the steel propeller shaft.
- Buckling load capacity of the propeller shaft made by Al6351, Al7075 or SM45C material is higher than their torque transmission capacity. Therefore, the design is safe under buckling load conditions.

## References

- [1] Lee D G, Kim H S, Kim J W and Kim J K 2004 *Compo. Struct.* **63** 87–99.
- [2] Taliban R, Ali A, Bedim A, Lehn A C and Golestaneh A F 2010 *Mat. Des.* **31** 514–521.
- [3] Cho D H, Lee D G and Choi J H 1997 *Compo. Struct.* **38** 309–319.
- [4] Kumar M and Kumar S M 2010 *Int. J. Moder. Eng. Res.* **3** 32–49.
- [5] Pater Z, Gontarz A, Tomczak J and Bulzak T 2015 *Arch. Civ. Mech. Eng.* **15** 917–924.
- [6] Rao B J, Srikanth D V, Kumar T S and Rao L S 2016 *Mat. Tod. Proc.* **3** 3673–3679.
- [7] Khalid Y A, Mutasher S A, Sahari B B and Hamouda A M S 2007 *Mat. Des.* **28** 329–334.
- [8] Zhang Z, Huang X and Hua H 2014 *J. Sou. Vib.* **333** 2608–2630.
- [9] Rangaswamy T, Ranjan S V, Chandrasekhar R A, Venkatesh T K and Anantharaman K 2004 *Mat. Sci. Eng.* **4** 2245–8745.
- [10] Kim M T, Kim D S and Oh O Y 2009 *Prog. Org. Coat.* **64** 281–286.
- [11] Rani M R and Rudramoorthy R 2013 *Ultrasoni.* **53** 763–772.
- [12] Mohanavel V, Rajan K, Senthil P V and Arul S 2017 *Mat. Tod. Proc.* **4** 3093–3101.
- [13] Chakherlou T N, Abazadeh B and Vogwell J 2009 *Eng. Failu. Analy.* **16** 242–253.
- [14] Raturi A, Mer K K S and Pant P K 2017 *Mat. Tod. Proc.* **4** 2645–2658.
- [15] Rompicharla R P K and Rambabu K 2012 *Int. J. Moder. Eng. Res.* **2** 3422–3428.